0022-3565/11/3362-372–380$20.00
THE JOURNAL OF PHARMACOLOGY AND EXPERIMENTAL THERAPEUTICS
JPET 336:372–380, 2011
Copyright © 2011 by The American Society for Pharmacology and Experimental Therapeutics
Vol. 336, No. 2
174102/3658981
Printed in U.S.A.

Pressor Effect of Apelin-13 in the Rostral Ventrolateral Medulla: Role of NAD(P)H Oxidase-Derived Superoxide

Fanrong Yao, Amit Modgil, Qi Zhang, Ajeeth Pingili, Neha Singh, Stephen T. O'Rourke, and Chengwen Sun

Department of Pharmaceutical Sciences, North Dakota State University, Fargo, North Dakota

Received August 17, 2010; accepted November 1, 2010

ABSTRACT

Microinjection of apelin-13 into the rostral ventrolateral medulla (RVLM) in the brainstem increases blood pressure in rats. In the present study, we tested the hypotheses that apelin-13 directly stimulates neuronal activity in neurons cultured from the brainstem and that NAD(P)H oxidase-derived reactive oxygen species are involved in this action of apelin-13. Microinjection of apelin-13 into the RVLM resulted in increases in arterial pressure and in renal sympathetic nerve activity in Sprague-Dawley rats. The pressor effect of apelin-13 was attenuated by the specific NAD(P)H-oxidase inhibitor gp91ds-tat. In neurons cultured from the ventral brainstem, spontaneous action potentials were recorded using current-clamp recording. Superfusion of neurons with apelin-13 (100 nM) increased the neuronal firing rate from 0.79 ± 0.14 to 1.45 ± 0.26 Hz ($n = 7$, $P < 0.01$) in angiotensin II receptor-like 1-positive neurons, identified with single-cell reverse transcriptase-polymerase chain reaction. Neither the angiotensin II type 1 receptor antagonist losartan nor the angiotensin II type 2 receptor antagonist 1-[[4-(dimethylamino)-3-methylphenyl[methyl]-5-(diphenylacetyl)-4,5,6,7-tetrahydro-1*H*-imidazo[4,5-*c*]pyridine-6-carboxylic acid ditrifluoroacetate (PD123319) altered the positive chronotropic effect of apelin-13. Pretreatment of cells with either the reactive oxygen species scavenger superoxide dismutase [polyethylene glycol-superoxide dismutase (PEG-SOD), 25 U/ml] or with gp91ds-tat significantly attenuated the chronotropic action of apelin-13. PEG-SOD and gp91ds-tat alone had no effect on basal neuronal firing. In addition, apelin-13 significantly increased NAD(P)H oxidase activity and elevated intracellular superoxide levels in neuronal cultures. The superoxide generator xanthine-xanthine oxidase also increased neuronal activity in neurons, mimicking the neuronal response to apelin-13. These observations provide the first evidence that apelin-13 directly increases neuronal activity via stimulation of NAD(P)H oxidase-derived superoxide, a cellular signaling mechanism that may be involved in the pressor effect of apelin-13 in the RVLM.

Introduction

Apelin was recently identified as an endogenous ligand of the APJ receptor, a G-protein-coupled receptor that shares 31% amino acid sequence identity with the angiotensin II type 1 (AT1) receptor (Tatemoto et al., 1998, Lee et al., 2000). Despite some homology between these receptors, apelin does not bind the AT1 receptor (O'Dowd et al., 1993). Multiple apelin peptides are derived from a 77-amino acid precursor peptide, preproapelin, and include apelin-36-(42–77), apelin-17-(61–77), and apelin-13-(65–77) (Masri et al., 2005). Apelin and its APJ receptors are widely distributed and mediate a variety of functions, including central and peripheral cardiovascular regulation, body fluid homeostasis, control of appetite, and possibly, immune function (Masri et al., 2005; Sorli et al., 2006). The structures of both apelin and its receptor are highly conserved between species, suggesting an important physiological role. The potent vasoactive and positive inotropic effects of apelin have drawn much attention in peripheral cardiovascular regulation (Szokodi et al., 2002; Berry et al., 2004; Ishida et al., 2004; Ashley et al., 2005). However, the central actions of this neuronal regulatory peptide on the cardiovascular system are not yet clarified.

In the brain, apelin-immunoreactive cell bodies or fibers,

This work was supported by the National Institutes of Health National Institute of Neurological Disorders and Stroke [Grant R21-NS055008] and the American Heart Association [Grant 10GRNT3170012]. Funding for the NDSU Core Biology Facility used in this study was from the National Institutes of Health National Center for Research Resources [Grant 2P20-RR015566].

Article, publication date, and citation information can be found at http://jpet.aspetjournals.org.

doi:10.1124/jpet.110.174102.

ABBREVIATIONS: APJ, angiotensin II receptor-like 1; AT1, angiotensin II type 1; AT2, angiotensin II type 2; AT1R, AT1 receptor; SON, supraoptic nucleus; RVLM, rostral ventrolateral medulla; NTS, nucleus tractus solitarius; SD, Sprague-Dawley; PBS, phosphate-buffered saline; RT-PCR, reverse transcriptase-polymerase chain reaction; ROS, reactive oxygen species; PEG, polyethylene glycol; SOD, superoxide dismutase; MAP, mean arterial pressure; DHE, dihydroethidium; RSNA, renal sympathetic nerve activity; PDHS, plasma-derived horse serum; DMEM, Dulbecco's modified Eagle's medium; ARC, cytosine arabinoside; BP, blood pressure; HR, heart rate; PD123319, 1-[[4-(dimethylamino)-3-methylphenyl [methyl]-5-(diphenylacetyl)-4,5,6,7-tetrahydro-1*H*-imidazo[4,5-*c*]pyridine-6-carboxylic acid ditrifluoroacetate.

preproapelin mRNA, and APJ receptor mRNA are distributed predominantly in neurons of the hypothalamus, brainstem, and other brain regions, including cardiovascular regulatory nuclei/areas, such as paraventricular nucleus, supraoptic nucleus (SON), nucleus tractus solitarius (NTS), and rostral ventrolateral medulla (RVLM) (De Mota et al., 2000; Lee et al., 2000; O'Carroll et al., 2000; Reaux et al., 2002). Accumulated evidence demonstrates that apelin regulates homeostasis and fluid balance via modulation of neuronal activity in the hypothalamus and alterations in the release of pituitary hormones, such as antidiuretic hormone and adrenocorticotropin (Lee et al., 2000; Taheri et al., 2002; De Mota et al., 2004). Recent electrophysiology studies performed in neurons of SON demonstrate that administration of apelin-13 stimulates neuronal firing rates and induces membrane potential depolarization but has no effect on oxytocin neurons (Tobin et al., 2008).

Apelin and APJ receptors are expressed in these cardiovascular regulatory regions in the brain (Hosoya et al., 2000), suggesting an important role in central regulation of blood pressure (O'Carroll et al., 2000; Reaux et al., 2001, 2002). Intracerebroventricular microinjections of apelin have been reported to either have no effect on blood pressure or result in a pressor response (Reaux et al., 2001; Kagiyama et al., 2005; Charles et al., 2006; Mitra et al., 2006). The reasons for the discrepant findings in these studies are not evident but may relate to differences in experimental methodologies. For example, the use of anesthetized versus conscious rats, the specific apelin peptide used, and variations in accessibility of apelin injected intracerebroventricularly to specific cardiovascular nuclei may contribute to the varying responses observed. It is even more interesting that microinjection of apelin into specific cardiovascular regulatory areas, such as the RVLM or NTS, increases blood pressure and sympathetic nerve activity (Seyedabadi et al., 2002). Our previous studies also demonstrate that microinjection of apelin-13 into the RVLM results in increases in arterial pressure, heart rate, and renal sympathetic nerve activity (Zhang et al., 2009). It is more noteworthy that viral vector-mediated overexpression of preproapelin in the RVLM induces a chronic elevation of blood pressure in conscious rats, which was associated with severe cardiac hypertrophy (Zhang et al., 2009). Despite increased awareness of the importance of apelin in the brainstem in blood pressure regulation, the cellular mechanisms underlying the pressor effect of apelin are still not clear. Thus, the objectives of the present study were 1) to determine the direct effect of apelin-13 on electrical activity in cultured neurons from ventral brain stem and 2) to determine the intracellular mechanisms underlying the neuronal response to apelin-13. In this study, we provide the first evidence that apelin-13 increases neuronal activity in neurons cultured from brainstem and that the chronotropic effect of apelin-13 is mediated by NAD(P)H oxidase-derived superoxide production. The NAD(P)H-derived superoxide is involved in the pressor response to apelin-13 microinjected into the RVLM.

Materials and Methods

Animals and Materials. One-day-old Sprague-Dawley (SD) rats used for neuronal culture preparations were obtained from our breeding colony, which originated from Charles River Laboratories (Wilmington, MA). Male adult SD rats (9–10 weeks old) used for in vivo studies were also purchased from Charles River Laboratories. Animal protocols were approved by the North Dakota State University Institutional Animal Care and Use Committee.

Dihydroethidium (DHE) was purchased from Invitrogen (Carlsbad, CA). DMEM was obtained from Invitrogen. Crystallized trypsin was from Worthington Biochemical (Freehold, NJ). Plasma derived horse serum (PDHS) was obtained from Central Biomedia (Irwin, MO). The selective NAD(P)H oxidase inhibitor gp91ds-tat ([H]RKKRRQRRR-CSTRIRRQL[NH_3]) and its control, scrambled gp91ds-tat ([H]RKKRRQRRR-CLRITRQSR[NH_3]), were synthesized by Tufts University Core Facility. Apelin-13, cytosine arabinoside (ARC), DNase 1, poly-L-lysine, ATP, GTP, HEPES, losartan, 1-[[4-(dimethylamino)-3-methylphenyl[methyl]-5-(diphenylacetyl)-4,5,6,7-tetrahydro-1*H*-imidazo[4,5-*c*]pyridine-6-carboxylic acid ditrifluoroacetate (PD123319), PEG-catalase, PEG-SOD, xanthine, xanthine oxidase, H_2O_2, and others were purchased from Sigma-Aldrich (St. Louis, MO).

Assessment of Renal Sympathetic Nerve Activity and BP. Male adult SD rats were anesthetized with a mixture of isoflurane (3%) and oxygen (1 l/min), which was delivered through a nose cone. PE-10 catheters fused to PE-50 catheters were prefilled with heparinized saline (100 IU/ml) and placed in the right femoral artery for acute recording of BP and HR. BP, HR, and assessment of renal sympathetic nerve activity (RSNA) data were collected and analyzed exactly as in our previous publication (Zhang et al., 2009).

RVLM Microinjection. Male adult SD rats were anesthetized with inhaled isoflurane as described above. The rats were placed in a stereotaxic frame (David Kopf Instruments, Tujunga, CA). Skin overlying the midline of the skull was incised, and a small hole was drilled bilaterally on the dorsal surface of the cranium according to the following coordinates: 1.9 mm lateral to the midline, 3.0 mm posterior to the lambdoid suture, and 10 mm below the outer surface of the skull. Multibarrel microinjection pipettes (tip size, 20–40 μm) were used for RVLM microinjection and were preloaded with different agents. One of the barrels was filled with a 5 μM solution of L-glutamate to confirm the BP-responsive site. The other barrels, depending on the experiment, contained saline, gp91ds-tat, or scrambled gp91ds-tat and apelin-13. The volume of microinjection (50 nl), as determined by the displacement of fluid meniscus in the micropipette-barrel, was visually confirmed under a modified binocular horizontal microscope. The duration of each injection was 5 to 10 s.

Preparation of Neuronal Cultures. Neuronal cultures were prepared from the brainstem RVLM region of 1-day-old rats as described previously (Sun et al., 2004). In brief, the cells were dissociated with trypsin (375 U/ml) and DNase I (496 U/ml), resuspended in DMEM containing 10% PDHS, and plated on poly-L-lysine–precoated 35-mm Nunc plastic tissue culture dishes. After cells were grown for 3 days at 37°C in humidified 95% O_2 and 5% CO_2, the culture medium was replaced with fresh DMEM containing ARC (1 μM) and 10% PDHS. After 2-day incubation, ARC was removed and the cells were incubated with normal medium for an additional 11 to 14 days before use. At the time of use, cultures consisted of 90% neurons and 10% astrocyte glia, as determined by immunofluorescent staining with antibodies against neurofilament proteins and glial fibrillary acidic protein (Sumners et al., 1990).

Electrophysiological Recordings. Spontaneous action potentials were recorded using the whole-cell patch-clamp technique in current-clamp mode, as described previously (Sun et al., 2004). In brief, cultured neurons (11–14 days old) were bathed in a solution containing 140 mM NaCl, 5.4 mM KCl, 2.0 mM $CaCl_2$, 2.0 mM $MgCl_2$, 0.3 mM NaH_2PO_4, 10 mM HEPES, 10 mM dextrose, and pH 7.4 (NaOH). Experiments were performed at room temperature (22–23°C) using an Axopatch-200B amplifier and a Digidata 1440A data acquisition system (Molecular Devices, Sunnyvale, CA). Data acquisition and analysis were performed using pClamp 10 software (Molecular Devices). Neurons in the culture dish (volume 1.5 ml) were superfused at a rate of 2 to 4 ml/min. Patch pipettes were pulled with a P-97 Flaming/Brown Micropipette Puller (Sutter Instrument, Novato, CA) and fire-polished to a final resistance of 2 to 5 MΩ. The

patch pipettes were filled with an internal pipette solution containing 140 mM KCl, 2 mM $MgCl_2$, 4 mM ATP, 0.1 mM guanosine 5-triphosphate, 10 mM dextrose, 10 mM HEPES, and pH 7.2 (KOH). The whole-cell configuration was formed by applying negative pressure to the patch electrode. The resting membrane potential was defined as the potential within a time period of 1 s, during which there was no spontaneous action potential firing. Neuronal firing rate was measured as the numbers of fully developed action potentials per second (in Hertz). In individual experiments, test agents were added sequentially in the superfusate.

It has been reported that APJ receptors are predominantly expressed in different cell populations (Tobin et al., 2008). The APJ receptor-positive neurons were identified with a single-cell RT-PCR technique, as published previously with minor modifications (Gómez-Lira et al., 2005). Glass patch pipettes for electrophysiological recordings were washed once in ethanol and three times in distilled water and then were autoclaved for 30 min. After electrophysiological recording as described above, the neuronal intracellular contents were drawn into the tip of the patch pipette using negative pressure. The procedure was performed carefully under a microscope equipped with a video monitoring system to avoid aspiration of the nucleus. The pipette tip was then broken off inside an RT-PCR tube containing 5 μl of RNase-free water, and RT-PCR was performed using a SuperScript III RT-PCR kit (Invitrogen). The RNA template from whole dishes was used as positive control, and the exclusion of RNA was used as negative control. The following primers were used to identify the APJ receptor: forward, 5′-TCCCTGCCATCTACATTCTGG-3′; reverse, 5′-GGCAAAGTCACCACAAAGGTC-3′. Messenger RNA from nonresponsive cells was also subjected to RT-PCR as a negative control.

The delayed rectifier K^+ current (I_{Kv}) was recorded using the whole-cell configuration of the patch-clamp technique with stepping from a holding potential of −40 to +10 mV. The I_{Kv} recording and data analysis was performed according to our methods published previously (Sun et al., 2003).

Measurement of Intracellular ROS Levels. Levels of reactive oxygen species were determined using the oxidant-sensitive fluorogenic probe DHE, essentially as described elsewhere (Zimmerman et al., 2002). In brief, primary cultured neurons were loaded with 100 nM DHE for 30 min at 37°C. The cells then were incubated with PBS for 5 min, followed by PBS containing apelin-13 (100 nM) for 5 min. In another set of neurons, cells were pretreated with gp91ds-tat (5 μM) or its control, scrambled gp91ds-tat, for 10 min before apelin-13 treatment to ensure complete inhibition of NAD(P)H oxidase. Ethidium fluorescence within neurons was detected by an Olympus fluorescence microscope equipped with a color digital camera, which was connected to a computer to capture and analyze images using Infinity Capture and Analyze Software (Lumenera Corporation, Ottawa, ON, Canada). Each treatment condition was run in triplicate within experiments, and each set of experiments was performed using three separate culture dishes.

Measurement of NAD(P)H Oxidase Activity. The NAD(P)H oxidase activity in neuronal cultures was measured using the lucigenin-derived chemiluminescence method, as described elsewhere (Li et al., 2002). Neuronal cultures were treated with apelin-13 (100 nM) or PBS for 5 min and washed in ice-cold PBS, and the cells then scraped and sonicated for 1 s. Ten minutes before recording luminescence, NAD(P)H (100 μM) and lucigenin (5 μM) were added and light emission was recorded during the next 10 s by a Microbetajet Luminometer (PerkinElmer Life and Analytical Sciences, Waltham, MA). Protein concentrations were determined using a Bio-Rad protein assay kit (Bio-Rad Laboratories, Hercules, CA) with bovine serum albumin standards. Data are presented as counts per minute per milligram of protein.

Data Analysis. All data are expressed as mean ± S.E. Comparisons for multiple experimental groups were performed using analysis of variance followed by Newman-Keuls correction, and Student's *t* test was performed for two-group comparisons. Differences were considered significant at $P < 0.05$.

Results

Gp91ds-tat, an NAD(P)H Oxidase Inhibitor, Attenuates the Central Effects of Apelin-13 In Vivo. We and others have demonstrated that apelin-13 microinjected into the RVLM results in increases in blood pressure and sympathetic outflow (Seyedabadi et al., 2002; Zhang et al., 2009). Thus, the objective in the first series of experiments was to establish the in vivo efficacy of gp91ds-tat to test the role of NAD(P)H oxidase-derived ROS in the pressor response to apelin-13. Microinjection of apelin-13 (200 pmol, 50 nl) into the RVLM increased MAP from 88 ± 9 to 115 ± 8 mm Hg (the changes in MAP are shown in Fig. 1C). Pretreatment with gp91ds-tat (2.5 nmol, 50 nl) attenuated the increases in MAP induced by apelin-13 (79% attenuation; Fig. 1, A–C). In contrast, pretreatment with scrambled gp91ds-tat (2.5 nmol, 50 nl) did not alter the pressor response of apelin-13 (MAP increase: 24 ± 4 versus 28 ± 4 mm Hg in control, $n = 7$, $P > 0.05$). In addition, pretreatment with gp91ds-tat (2.5 nmol, 50 nl) significantly attenuated apelin-13-induced increases in HR (apelin-13: 40 ± 4 bpm versus apelin-13 plus gp91ds-tat: 7 ± 4 bpm, $n = 7$, $P < 0.05$). The same dose of scrambled gp91ds-tat had no effect on apelin-13-induced increases in HR (Fig. 1, A and D). Microinjection of gp91ds-tat or scrambled gp91ds-tat alone into the RVLM did not alter either MAP or HR. We also examined the effect of gp91ds-tat on the sympathetic activation produced by microinjection of apelin-13 into the RVLM. RVLM microinjection of apelin-13 resulted in a 23 ± 3% increase in RSNA, and pretreatment with gp91ds-tat (2.5 nmol, 50 nl) significantly attenuated the apelin-13-induced increase in RSNA by 79%. In contrast, pretreatment with scrambled gp91ds-tat (2.5 nmol, 50 nl) did not alter the sympathetic response to apelin-13 (Fig. 1, A, B, and E). However, microinjection of either gp91ds-tat or scrambled pg91ds-tat alone into the RVLM had no effect on RSNA. These data suggest collectively that NAD(P)H oxidase-derived ROS are involved in the central actions of apelin-13 in the regulation of blood pressure and sympathetic outflow.

Apelin-13 Reversibly Increases Neuronal Firing Rate. We next examined the effect of apelin-13 on neuronal activity in cultured neurons using the patch-clamp technique, as detailed under *Materials and Methods*. Superfusion of neurons with apelin-13 (100 nM) produced a rapid increase in firing rate from a control level of 0.79 ± 0.14 to 1.45 ± 0.26 Hz ($n = 7$, $P < 0.01$) in APJ receptor-positive neurons, identified by single-cell RT-PCR (Fig. 2, A and B). However, the same concentration of apelin-13 had no effect on neuronal firing rate in APJ receptor-negative neurons (0.76 ± 0.12 and 0.75 ± 0.14 Hz before and after administration of apelin-13, $n = 6$, $P > 0.05$). The apelin-13-induced chronotropic action was readily reversed upon washing out (Fig. 2, A and B). The response to apelin-13 was rapid, reaching a peak in 5 min, and lasted for the duration of time that apelin-13 was applied (Fig. 2E). These data suggest that apelin-13 induces a positive chronotropic effect via an APJ receptor-mediated mechanism and that the response to apelin-13 is reversible.

It has been reported that the APJ receptor has a 31% amino acid sequence homology with the angiotensin II type 1

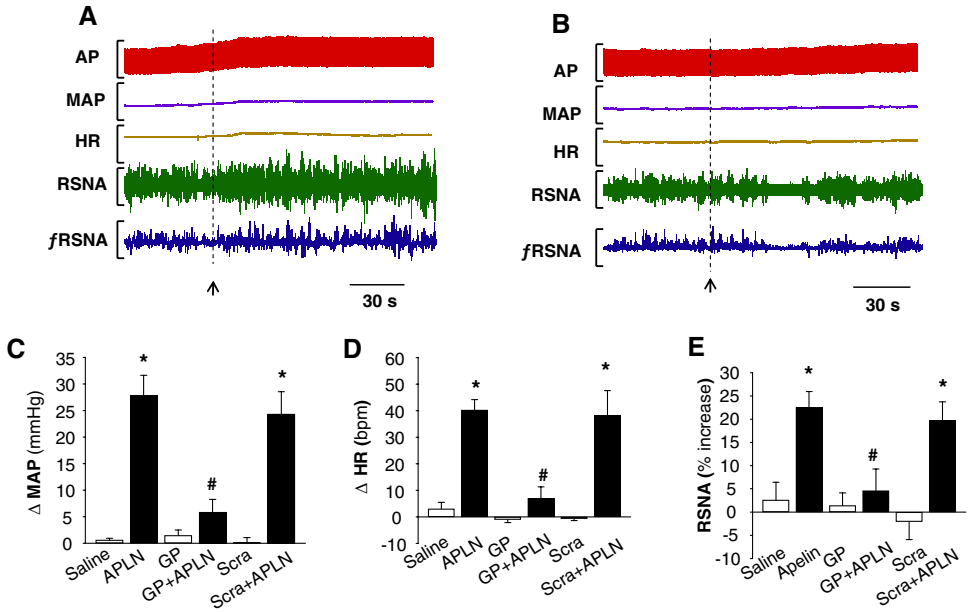

Fig. 1. Role of NAD(P)H oxidase in the pressor response to apelin-13 microinjected in the RVLM. A and B, representative tracings showing arterial pressure (AP), MAP, HR, RSNA, and integrated RSNA (*f*RSNA) before and after microinjection of apelin-13 (200 pmol, 50 nl) into the RVLM of SD rats pretreated with scrambled gp91ds-tat (Scra, 2.5 nmol, 50 nl, 18 min) (A) or NADPH oxidase inhibitor gp91ds-tat (GP, 2.5 nmol, 50 nl, 18 min) (B). C, bar graphs summarizing the change of MAP (ΔMAP) induced by RVLM microinjection (50 nl) of saline, apelin-13 (APLN, 200 pmol), gp91ds-tat (GP, 2.5 nmol), GP plus apelin-13 (GP+APLN), scrambled gp91ds-tat (Scra, 2.5 nmol), and scrambled gp91ds-tat plus apelin-13 (Scra+APLN). Data are means ± S.E. (n = 5 to 7 rats in each group). ∗, $P < 0.01$ significant difference compared with respective control. #, $P < 0.05$ versus APLN. D, bar graphs summarizing the change of heart rate (ΔHR) induced by RVLM microinjection of agents described in C. Data are means ± S.E. (n = 5 to 7 rats in each group). ∗, $P < 0.01$ significant difference compared with respective control. #, $P < 0.05$ versus APLN. E, bar graphs summarizing the percentage increases of RSNA after RVLM microinjection of agents described in C. Data are means ± S.E. (n = 5 to 7 rats in each group). ∗, $P < 0.01$ significant difference compared with respective control. #, $P < 0.05$ versus apelin-13 (APLN).

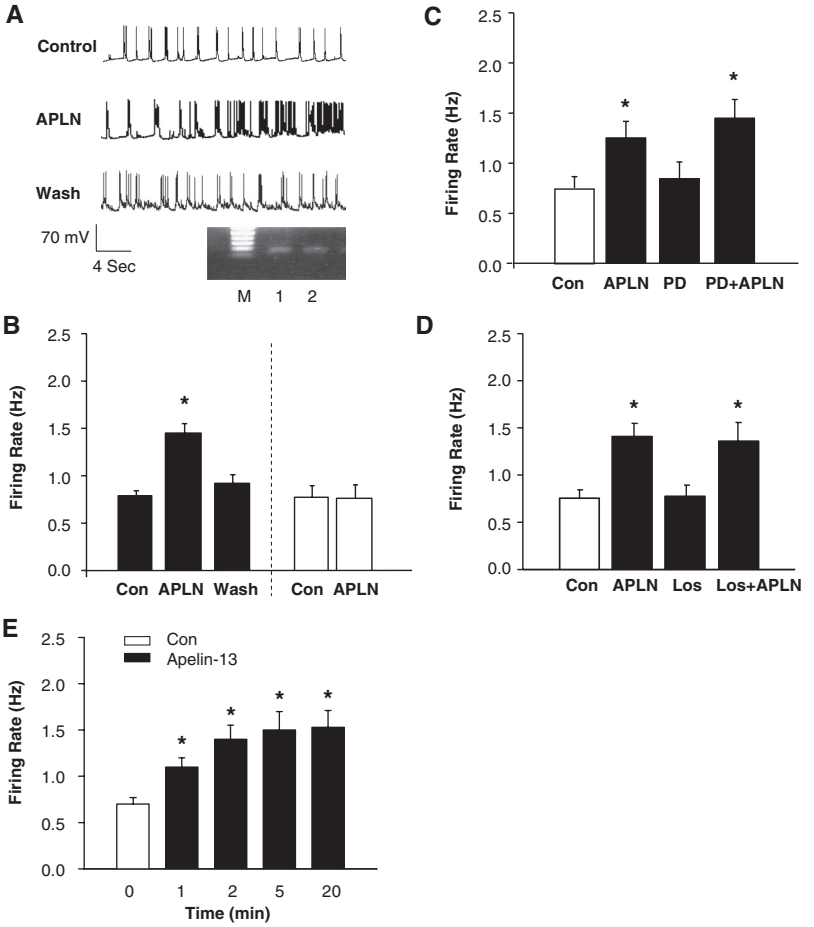

Fig. 2. Apelin-13 exerts a positive chronotropic action via an AT1 receptor- and AT2 receptor-independent mechanism. A, representative recordings showing spontaneous neuronal action potentials recorded under the following conditions: superfusion of control solution (PBS), superfusion of apelin-13 (APLN, 100 nM), and followed by washing with superfusate solution. Action potentials were recorded from an APJ receptor-positive neuron identified by single-cell RT-PCR. Ethidium bromide-stained gels, seen in A, show the PCR DNA products that correspond to APJ receptor mRNA obtained from the same neuron after electrophysiological recordings (lane 2). The RNA from the whole dish of neurons was used as positive control (lane 1). M, marker. B, bar graph summarizing the effect of apelin-13 on the neuronal firing rate recorded from APJ receptor-positive neurons (filled bars) or APJ receptor-negative neurons (open bars) identified by RT-PCR. Data are means ± S.E. (n = 7, 6). ∗, $P < 0.01$ compared with Con. C, effect of apelin-13 on neuronal firing rate under the following sequential treatment conditions: superfusion with control (Con) solution (PBS), superfusion with apelin-13 (APLN, 100 nM), wash with superfusate solution, superfusion with PD123319 (PD, 1 μM), and combined application of apelin-13 and PD123319 (PD+APLN). Data are mean ± S.E. from seven neurons. ∗, $P < 0.01$ compared with Con. D, bar graphs of the firing rate recorded in each treatment condition as described in C, with the exception of PD123319, which was replaced with losartan (Los, 1 μM). Data are mean ± S.E. from seven neurons. ∗, $P < 0.01$ versus respective control treatment. E, time-dependent response of neuronal firing to apelin-13. The neuronal firing was recorded in neurons treated with apelin-13 (100 nM) for the time periods indicated in the graph. Results are mean ± S.E.; n = 6. ∗, $P < 0.05$ compared with Con.

(AT1) receptor (Lee et al., 2000) and that both AT1 and angiotensin II type 2 (AT2) receptors are expressed in these neuronal cultures (Sumners et al., 1990). Thus, we determined the effects of the AT1 receptor antagonist losartan and the AT2 receptor antagonist PD123319 on the chronotropic action of apelin-13 in rat neurons to examine the possibility of whether there are interactions between the angiotensin system and apelin system with regard to neuronal activity. Figure 2C demonstrates that superfusion of neuronal cultures with apelin-13 (100 nM) produced the expected increases in firing rate (from 0.72 ± 0.11 to 1.20 ± 0.16 Hz, $n = 7$, $P < 0.01$) and that superfusion of these cells with 1 μM PD123319 did not significantly alter basal firing rate (Fig. 2C). In the presence of PD123319, apelin-13 (100 nM) still produced a significant increase in firing rate (from 0.81 ± 0.16 to 1.39 ± 0.18 Hz, $n = 7$, $P < 0.05$). We next examined the effect of losartan on the chronotropic effect of apelin-13; the results are shown in Fig. 2D, demonstrating that losartan (1 μM) did not significantly alter the increase in neuronal firing rate produced by apelin-13 (100 nM). The results are shown in Fig. 2, C and D, demonstrating that pretreatment of neurons with neither losartan (1 μM) nor PD123319 (1 μM) altered the neuronal response to apelin-13. Both losartan and PD123319 had no effect on basal neuronal activity (Fig. 2, C and D). In a separate set of control experiments, neuronal responses to sequentially administrated apelin-13 were determined. Superfusion of neurons with apelin-13 (100 nM) increased neuronal firing rate by 81 ± 9% ($n = 5$, $P < 0.05$). Neuronal firing was reduced to the basal control level after washing out apelin-13, and when followed by superfusion of the same neuron with apelin-13 (100 nM), neuronal firing rate was increased by 85 ± 7% ($n = 5$, $P < 0.05$), indicating that there is no significant difference between the two responses to apelin-13 ($n = 5$, $P > 0.05$). Taken together, these data indicate that apelin-13 increased neuronal firing rate via an AT1 receptor- and AT2 receptor-independent mechanism in neurons.

Apelin-13 Increase ROS Production in Neurons. The fluorogenic probe, DHE, was used to assess the effect of apelin-13 on ROS production in primary cultured neurons. Under control conditions, ethidium fluorescence was low in PBS-treated neurons (Fig. 3B); however, treatment of these same cells with apelin-13 (100 nM) resulted in a significant increase in the intensity of ethidium fluorescence within neurons (443.7 ± 15.2 and 782.1 ± 30.2 ethidium fluroresence intensity of cells treated with control PBS and with apelin-13, $n = 20$ neurons, $P < 0.01$; Fig. 3, B, C, and G). The apelin-13-induced increase in ethidium fluorescence was abolished by gp91ds-tat (5 μM) (442.2 ± 19.3 and 477.3 ± 33.1 ethidium fluorescence intensity of cells treated with gp91ds-tat and gp91ds-tat+apelin-13, respectively, $n = 15$, $P > 0.05$; Fig. 3, E, F, and H). However, the scrambled control gp91ds-tat did not alter the stimulatory action of apelin on ROS production (439.0 ± 20.1 and 809.0 ± 44.9 ethidium

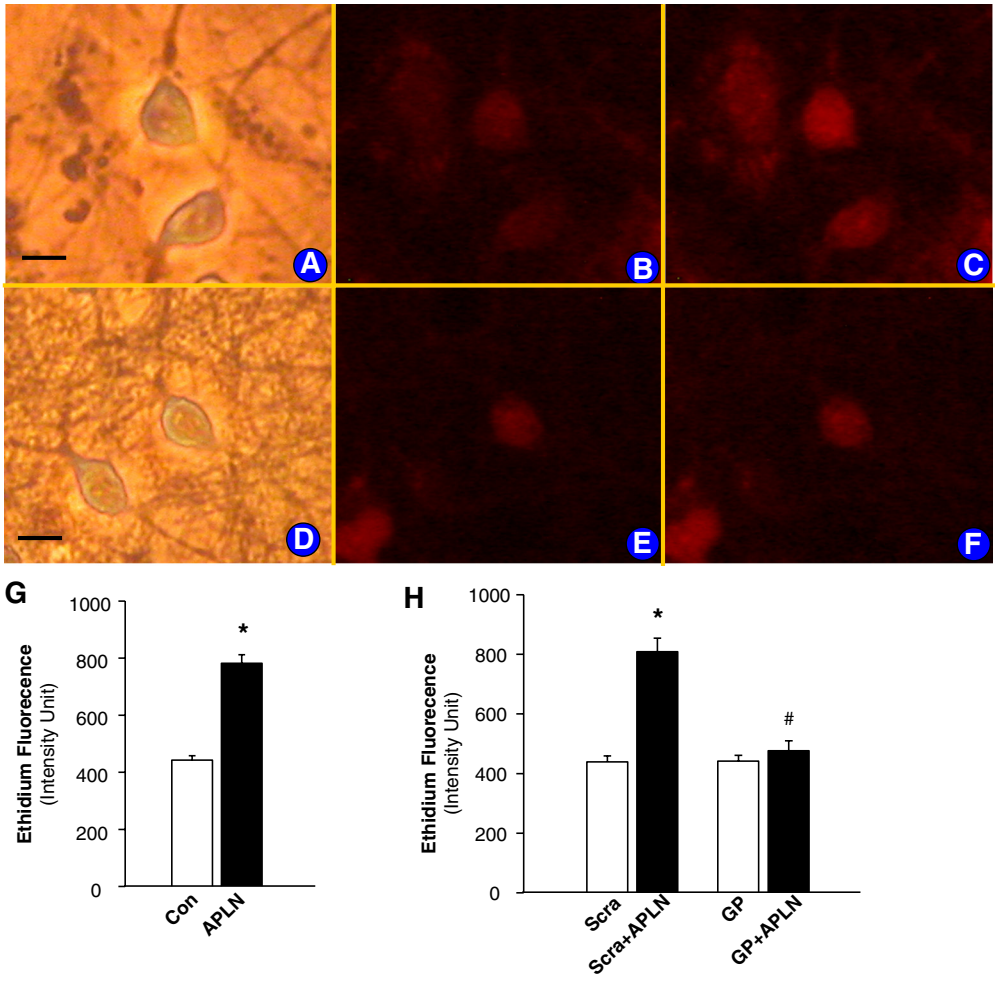

Fig. 3. Effect of apelin-13 on neuronal ROS production. ROS levels were detected using the fluorogenic probe, DHE, as described under *Materials and Methods*. A to C, neurons that were treated under the following conditions: neurons in normal optical phase (A); fluorescence micrograph of the same neurons in A, loaded with DHE (B); and fluorescence micrograph of neurons treated with apelin-13 (100 nM) (C). Bar = 10 μm. D to F, neurons that were treated under the following conditions: neurons in normal optical phase (D); fluorescence micrograph of the same neurons in D treated with gp91ds-tat (GP, 5 μM) (E); and fluorescence micrograph of neurons treated with GP plus apelin-13 (100 nM) (F). G, bar graphs summarizing ethidium fluorescence intensity before and after treatment with apelin-13 (APLN, 100 nM). Data are mean ± S.E.; fluorescence intensity from 20 neurons in each group. They are derived from three experiments and at least three dishes in each experiment. H, bar graphs summarizing fluorescence intensity before and after treatment with apelin-13 (APLN, 100 nM) in the presence of GP (5 μM) or scrambled-gp91ds (Scra, 5 μM). Data are mean ± S.E. ($n = 15$ neurons in each group). *, significantly different from control (PBS, $P < 0.01$). #, significantly different from cells treated with apelin-13 plus scrambled control ($P < 0.05$).

fluorescence intensity of cells treated with scrambled gp91ds-tat and scrambled gp91ds-tat+apelin-13, respectively, $n = 15$, $P < 0.01$). These results indicate that apelin-13 increases superoxide production, which is blocked by inhibition of NAD(P)H oxidase. It has been determined in a previous study (Sumners et al., 1990) that the neuronal cultures used in this experiment contain approximately 90% neurons and 10% astrocyte glia. Thus, we also determined the effect of apelin-13 on the intracellular ROS levels in primarily cultured glial cells, which were identified by immunofluorescent staining with antibodies against glial fibrillary acidic protein. Treatment of glial cells with apelin-13 (1 nM) did not significantly alter the ethidium fluorescence intensity (483.4 ± 19.8 in control versus 492.7 ± 22.1 in apelin-13 treatment, $n = 19$ cells in each group, $P > 0.05$), indicating that apelin-13 has less effect on ROS production in brain glial cells compared with neurons.

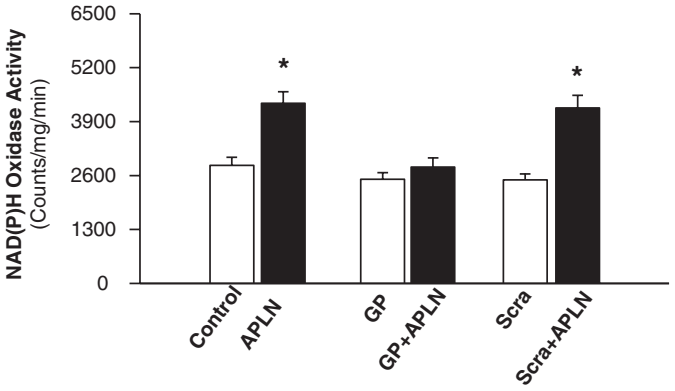

Fig. 4. Effect of apelin-13 and gp91ds-tat on neuronal NAD(P)H oxidase activity. Neuronal cultures were pretreated with control (Con, PBS), gp91ds-tat (GP, 5 μM), or scrambled gp91ds (Scra, 5 μM) for 10 min before treatment with apelin-13 (APLN, 100 nM). Neurons were collected, and NAD(P)H oxidase activity was measured and expressed as mean light emission (count per milligram of protein per minute). Data are mean ± S.E. ($n = 8$). *, significantly different from PBS control ($P < 0.05$).

Apelin-13 Stimulates NAD(P)H Oxidase in Neuronal Cultures. Treatment of primary cultured neurons with apelin-13 (100 nM) resulted in a 2-fold increase in NAD(P)H oxidase activity (Fig. 4). This effect of apelin was completely blocked by preincubation of neurons with gp91ds-tat (5 μM). However, pretreatment of neurons with the scrambled gp91ds-tat (5 μM) did not significantly alter the apelin-13-induced response to NAD(P)H oxidase (Fig. 4). These data demonstrate that apelin-13 stimulates NAD(P)H oxidase activity in neuronal cultures and that this effect of apelin-13 is blocked completely by gp91ds-tat.

NAD(P)H Oxidase-Derived ROS Are Involved in the Chronotropic Effect of Apelin-13. In this series of experiments, we investigated the role of NAD(P)H oxidase in the apelin-induced increase in neuronal firing rate. Similar to the data in Fig. 1, apelin-13 (100 nM) induced a significant increase in neuronal firing rate in most neurons (neurons that failed to respond to apelin-13 were not included in the analysis). In apelin-13-responsive neurons, washout of apelin-13 for 10 to 15 min returned firing rate to baseline levels, and superfusion with gp91ds-tat (5 μM) alone did not alter firing rate (Fig. 5, A and C). Subsequent superfusion of apelin-13 (100 nM) in the presence of gp91ds-tat attenuated the chronotropic effect of apelin-13 (Fig. 5, A and C). In contrast, scrambled gp91ds-tat (5 μM) did not significantly alter the apelin-13-induced chronotropic effect under the same treatment conditions (Fig. 5, B and C). Neither gp91ds-tat nor scrambled gp91ds-tat alone had any significant effect on basal neuronal activity. In summary, these results demonstrate that the apelin-13-induced increase in neuronal firing rate is mediated by NAD(P)H oxidase-derived ROS production in neurons.

Superoxide Contributes to the Chronotropic Effect of Apelin-13. To identify whether superoxide contributes to the positive chronotropic effect of apelin13, we examined the chronotropic action of apelin-13 in the presence or absence of a cell-permeable superoxide scavenger, PEG-SOD (25 U/ml). Protocols similar to those used in the above gp91ds-tat ex-

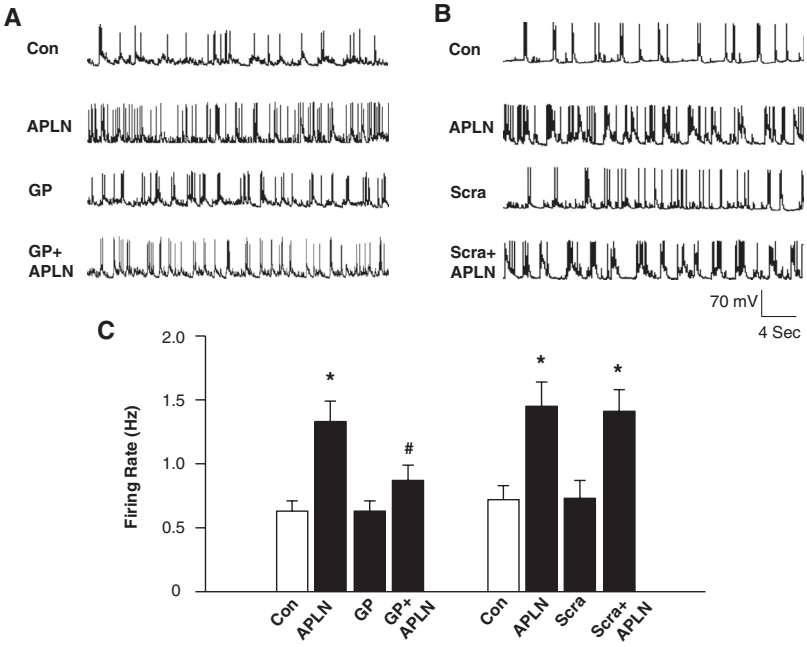

Fig. 5. Effect of gp91ds-tat on the chronotropic action of apelin-13 in neurons. A and B, representative recordings of action potentials from rat cultured neurons under the following sequential treatment conditions: perfusion of PBS control (Con), followed by superfusion of apelin-13 (APLN, 100 nM), washout of apelin-13 with fresh superfusate solution, superfusion of scrambled gp91ds-tat (Scra, 5 μM), or gp91ds-tat (GP, 5 μM); superfusion of apelin-13 plus gp91ds-tat (APLN+GP) or scrambled gp91ds-tat (APLN+Scra). C, bar graphs summarizing the effects of gp91ds-tat on the chronotropic action of apelin-13 in neurons. Data are mean ± S.E. ($n = 6$–7 neurons). *, $P < 0.01$ compared with respective control recordings. #, $P < 0.05$ compared with apelin-13 treatment. Scrambled gp91ds-tat (5 μM) or gp91ds-tat (5 μM) alone had no significant effects on basal firing rate.

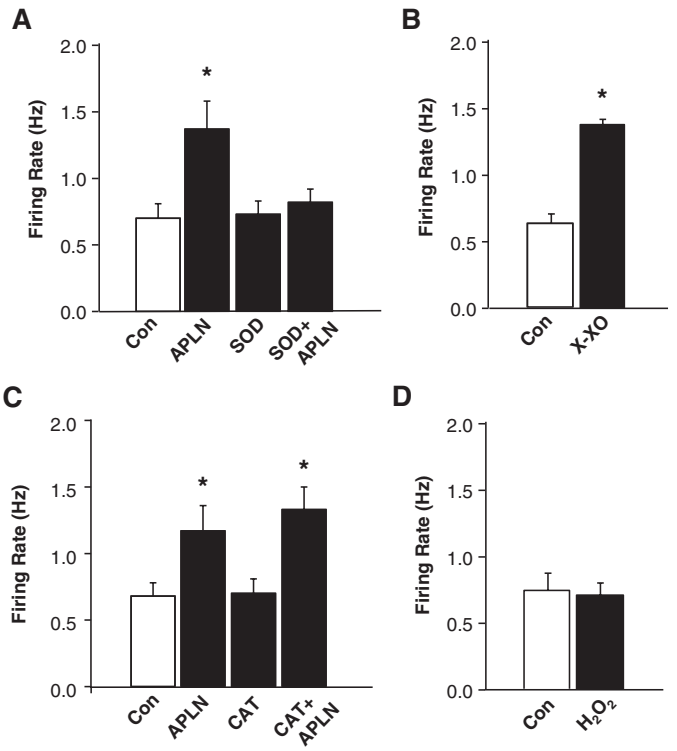

Fig. 6. Identification of ROS involved in the chronotropic actions of apelin-13 in neurons. A, role of superoxide. The neuronal firing rate was recorded in neurons treated under the following conditions: superfusion of PBS control (Con); superfusion of apelin-13 (APLN, 100 nM) followed by washout of apelin-13 with fresh superfusate solution; superfusion of PEG-SOD (SOD, 25 U/ml), and PEG-SOD plus apelin-13 (SOD+APLN). Data are mean ± S.E. (n = 9 neurons). B, effect of xanthine-xanthine oxidase on neuronal firing rate. The neuronal firing rate was recorded in neurons treated under PBS control (Con) and superfusion of xanthine-xanthine oxidase (10 mM and 20 mU/ml). Data are mean ± S.E. (n = 5 neurons). C, role of hydrogen peroxide. The neuronal firing rate was recorded in neurons treated under the following conditions: superfusion of PBS control (Con); superfusion of apelin-13 (APLN, 100 nM) followed by washout of apelin-13 with fresh superfusate solution, superfusion of PEG-catalase (CAT, 250 U/ml), and PEG-catalase plus apelin-13 (CAT+APLN). Data are mean ± S.E. (n = 7 neurons). D, effect of hydrogen peroxide on neuronal firing rate. Data are mean ± S.E. of neuronal firing rate in eight neurons treated under PBS control (Con) and superfusion of hydrogen peroxide (H_2O_2, 1 μM). *, $P < 0.05$ compared with respective control.

periments were followed. Superfusion of neurons with apelin-13 (100 nM) triggered a significant increase in neuronal firing rate (Fig. 6A). This chronotropic action of apelin-13 was attenuated by pretreatment of the neurons with PEG-SOD (25 U/ml). PEG-SOD alone had no effect on the basal neuronal firing rate. Moreover, superfusion of neurons with a superoxide generator, xanthine-xanthine oxidase (10 mM and 20 mU/ml), increased neuronal firing rate (from 0.63 ± 0.07 to 1.38 ± 0.04 Hz, n = 5 neurons, $P < 0.05$), mimicking the effects of apelin-13 (Fig. 6B). These results suggest that superoxide is involved in the apelin-13-induced increase in neuronal firing rate in SD rat neurons. We next examined the role of hydrogen peroxide (H_2O_2) in the chronotropic action of apelin-13. Pretreatment of cells with a cell-permeable H_2O_2 scavenger, PEG-catalase (250 U/ml), did not significantly alter the apelin-induced increase in neuronal firing rate (Fig. 6C). Superfusion of neurons with H_2O_2 (1 μM) had no significant effect on basal neuronal firing (0.74 ± 0.13 and 0.71 ± 0.09 Hz in the neurons treated with control PBS and H_2O_2, n = 8 neurons, $P > 0.05$; Fig. 6D). Taken together, these data suggest that the positive chronotropic effect of apelin-13 is mediated by intracellular superoxide production in rat neurons.

Apelin-13 Inhibits I_{Kv} via a NADPH Oxidase-Dependent Mechanism. Both K^+ and Ca^{2+} currents contribute to action potential formation, and alterations in the activity of these ion channels modulate the frequency of action potentials, thereby changing neuronal firing. Because ROS have been linked to alterations in K^+ and Ca^{2+} currents (Sun et al., 2003; Wang et al., 2004; Yin et al., 2010), we next examined the effect of apelin-13 on I_{Kv} and the role of NADPH oxidase-derived ROS in this action of apelin-13 on I_{Kv} in cultured rat neurons. We recorded I_{Kv} using voltage steps from −40 to +10 mV in the whole-cell patch-clamp mode. The results are shown in Fig. 7, demonstrating that treatment of neurons with apelin-13 significantly inhibited I_{Kv} and that this inhibitory effect of apelin-13 was reversed completely by pretreatment with 5 μM gp91ds-tat. However, the same dose of scrambled gp91ds-tat did not alter the effect of apelin-13 on I_{Kv} in cultured rat neurons. These data demonstrate that the ROS-mediated chronotropic action of apelin-13 may involve inhibition of I_{Kv}.

Discussion

The important new findings of this study are that NAD(P)H oxidase-derived ROS are involved in the pressor response to apelin-13 microinjected into the RVLM in normotensive rats and that apelin-13 increases RVLM neuronal activity, an effect that is mediated by NAD(P)H oxidase-derived ROS. These conclusions are supported by the following observations: 1) inhibition of NAD(P)H oxidase attenuated increases in arterial pressure, heart rate, and renal sympathetic nerve activity resulting from microinjection of apelin-13 into the RVLM of normotensive rats; 2) apelin-13 increased spontaneous neuronal firing exclusively in APJ-receptor-positive neurons via an AT1R- and AT2R-independent mechanism; 3) the chronotropic effect of apelin-13 was attenuated by blockade of NAD(P)H oxidase or by the superoxide scavenger PEG-SOD; 4) incubation of neurons with apelin-13 increased intracellular superoxide levels and NAD(P)H oxidase activity; and 5) superfusion of neurons with a superoxide generator, xanthine-xanthine oxidase, also increased neuronal activity, mimicking the action of apelin-13.

APJ receptors and apelin are found in a variety of brain areas, including hypothalamus and brainstem. In the hypothalamus, the most intense expression of the apelin/APJ receptor system is in the SON and paraventricular nuclei (De Mota et al., 2000; Lee et al., 2000; O'Carroll et al., 2000; Reaux et al., 2002). Therefore, it is proposed that apelin regulates fluid homeostasis and appetite by changing neuronal activity in these brain areas to control secretion of a variety of hormones, such as vasopressin and adrenocorticotropin (Lee et al., 2000; Taheri et al., 2002; De Mota et al., 2004). This is supported by recent observations demonstrating that apelin-13 directly increases neuronal firing rate and induces membrane depolarization in vasopressin-containing cells isolated from the SON (Tobin et al., 2008). However, the second messenger signaling system(s) involved in the apelin/APJ receptor-mediated response in neurons is not yet fully understood. The results of the current study demonstrate

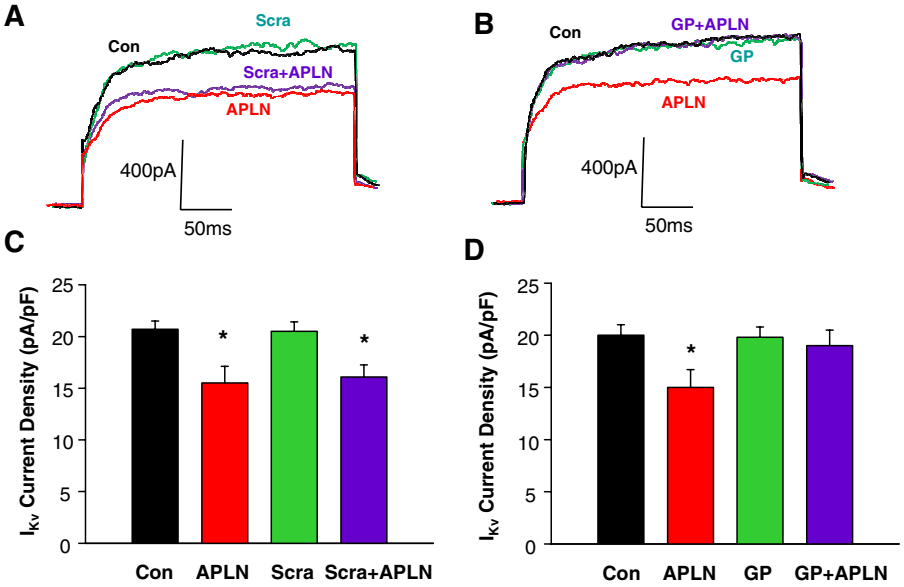

Fig. 7. Effect of apelin-13 and NADPH oxidase inhibitors on neuronal delayed rectifier K^+ current (I_{Kv}). I_{Kv} was recorded during 250-ms voltage steps from a holding potential of −40 to +10 mV. A and B, representative current tracings of neuronal I_{Kv} recorded from neurons under the following sequential treatment conditions: control (Con), superfusion of apelin-13 (100 nM), washout of apelin-13, superfusion of gp91ds-tat (GP, 5 μM) or scrambled gp91ds-tat (Scra, 5 μM), and superfusion of apelin-13 plus GP or Scra. C and D, bar graphs show mean ± S.E. of I_{Kv} densities obtained in each treatment condition described in A and B. n = 8 and 6 neurons for GP and Scra group, respectively; *, $P < 0.05$ compared with control.

that apelin-13 also increases neuronal activity in neurons cultured from the ventral brainstem RVLM area and that the chronotropic action of apelin-13 is mediated by NAD(P)H oxidase-dependent superoxide production within these neurons. Treatment of neurons with apelin-13 increased NAD(P)H oxidase activity and elevated intracellular ROS levels by a NAD(P)H oxidase-dependent mechanism. Furthermore, selective blockade of NAD(P)H oxidase or scavenging superoxide attenuated the chronotropic effect of apelin-13. These results are consistent with previous observations in APJ receptor knockout mice, in which oxidative stress-linked atherosclerosis was prevented (Hashimoto et al., 2007). In addition, apelin-induced cell proliferation was attenuated by treatment with SOD or the NAD(P)H oxidase inhibitor diphenylene iodonium in cultured vascular smooth muscle cells (Hashimoto et al., 2007). Taken together, the evidence strongly suggests that an NAD(P)H oxidase/superoxide-dependent mechanism may be a crucial signaling mechanism in the action of the apelin/APJ receptor system in neurons within the RVLM.

It has been reported that intracerebroventricular application of apelin-13 increased blood pressure and heart rate in conscious animals and that pretreatment with intracerebroventricular injection of an AT1R antagonist did not alter these responses to apelin (Charles et al., 2006). In addition, Seyedabadi et al. (2002) reported that microinjection of apelin-13 directly into the NTS and RVLM elicited an increase in arterial pressure, suggesting that the brainstem may be a primary site of action in the pressor effect of apelin-13. Consistent with these in vivo studies, the current experiments provide direct evidence that exposure to apelin-13 increases neuronal firing in neurons cultured from ventral brainstem RVLM area. These observations suggest that the pressor effect of apelin-13 may be mediated by the direct stimulation of neurons within the brainstem. In accordance with the previous finding that the APJ receptor has 31% homology with the AT1 receptor, we tested whether the apelin-13-induced increase in neuronal firing is mediated via AT1 receptors. Pretreatment of neurons with the AT1 receptor antagonist losartan did not change the chronotropic effect of apelin-13, suggesting that the actions of apelin-13 on neurons are independent of AT1 receptors.

The present observations demonstrate that apelin-13 increases intracellular superoxide levels by stimulating NAD(P)H oxidase and that increased superoxide production is involved in the chronotropic action of apelin-13 in rat brainstem neurons. Although superoxide may be rapidly converted to hydrogen peroxide, it is unlikely that the chronotropic effect of apelin-13 is mediated by hydrogen peroxide because the hydrogen peroxide scavenger, catalase, had no effect on the response to apelin-13, and authentic hydrogen peroxide itself had no effect on neuronal firing rate. These results are supported by data from studies in vascular smooth muscle cells showing that NAD(P)H oxidase-dependent superoxide production is involved in the apelin-13-induced increase in vascular smooth muscle cell proliferation (Hashimoto et al., 2007). However, the nature of the intracellular signaling mechanisms by which superoxide increases neuronal firing rate in neurons remains to be clarified. One possibility may be a direct redox-dependent regulation of ion channel activity. The current study demonstrated that apelin-13 inhibited K^+ channel currents and that the inhibitory effect of apelin-13 was attenuated by an NAD(P)H oxidase inhibitor. These data strongly suggest that the underlying cellular mechanism of action of apelin involves inhibition of neuronal K^+ channel currents; however, we cannot exclude a role for Ca^{2+} channels in the action of apelin-13 and ROS on the regulation of neuronal activity. It has been reported that apelin-13 stimulates Ca^{2+} currents in vasopressin neurons (Tobin et al., 2008) and that the pore-forming subunit of Ca^{2+} channel contains more than 10 cysteine residues (Mikami et al., 1989) that can potentially undergo redox modification. Thus, the precise role of specific ion channels in the actions of superoxide and apelin-13 will require further investigation.

In the current study, we also observed the time course of the neuronal response to apelin-13 in cultured neurons. The response to apelin-13 was rapid, reaching a peak in 5 min and lasting at least 20 min. In contrast, our previous study demonstrated that the pressor effect of apelin-13 microinjected into the RVLM of rats started at 2 min, peaked at 4 to 10 min, and lasted only approximately 14 min. The reason for the shorter duration of action of apelin-13 in vivo is not clear. One possible explanation may be that apelin-13 is rapidly degraded in this brain area, which could decrease the activity

of the peptide when microinjected during in vivo experiments. Indeed, angiotensin-converting enzyme 2, an enzyme that hydrolyzes both apelin and angiotensin II with similar potency, is highly expressed in the RVLM (Yamazato et al., 2007) and, therefore, is responsible for the degradation of both peptides.

In summary, the novel neurohormonal peptide, apelin-13, increases neuronal activity via an AT1 receptor-independent mechanism in neurons. The positive chronotropic action of apelin-13 is mediated by NAD(P)H oxidase-derived superoxide accumulation in neurons and may contribute to the regulation of cardiovascular function and blood pressure by this peptide.

Authorship Contributions

Participated in research design: O'Rourke and Sun.

Conducted experiments: Yao, Modgil, Zhang, Pingili, and Singh.

Performed data analysis: Yao, Modgil, Zhang, Pingili, and Singh.

Wrote or contributed to the writing of the manuscript: O'Rourke and Sun.

Other: Sun acquired funding for this research.

References

Ashley EA, Powers J, Chen M, Kundu R, Finsterbach T, Caffarelli A, Deng A, Eichhorn J, Mahajan R, Agrawal R, et al. (2005) The endogenous peptide apelin potently improves cardiac contractility and reduces cardiac loading in vivo. *Cardiovasc Res* **65:**73–82.

Berry MF, Pirolli TJ, Jayasankar V, Burdick J, Morine KJ, Gardner TJ, and Woo YJ (2004) Apelin has in vivo inotropic effects on normal and failing hearts. *Circulation* **110:**II187–II193.

Charles CJ, Rademaker MT, and Richards AM (2006) Apelin-13 induces a biphasic haemodynamic response and hormonal activation in normal conscious sheep. *J Endocrinol* **189:**701–710.

De Mota N, Lenkei Z, and Llorens-Cortès C (2000) Cloning, pharmacological characterization and brain distribution of the rat apelin receptor. *Neuroendocrinology* **72:**400–407.

De Mota N, Reaux-Le Goazigo A, El Messari S, Chartrel N, Roesch D, Dujardin C, Kordon C, Vaudry H, Moos F, and Llorens-Cortes C (2004) Apelin, a potent diuretic neuropeptide counteracting vasopressin actions through inhibition of vasopressin neuron activity and vasopressin release. *Proc Natl Acad Sci USA* **101:** 10464–10469.

Gómez-Lira G, Lamas M, Romo-Parra H, and Gutiérrez R (2005) Programmed and induced phenotype of the hippocampal granule cells. *J Neurosci* **25:**6939–6946.

Hashimoto T, Kihara M, Imai N, Yoshida S, Shimoyamada H, Yasuzaki H, Ishida J, Toya Y, Kiuchi Y, Hirawa N, et al. (2007) Requirement of apelin-apelin receptor system for oxidative stress-linked atherosclerosis. *Am J Pathol* **171:**1705–1712.

Hosoya M, Kawamata Y, Fukusumi S, Fujii R, Habata Y, Hinuma S, Kitada C, Honda S, Kurokawa T, Onda H, et al. (2000) Molecular and functional characteristics of APJ. Tissue distribution of mRNA and interaction with the endogenous ligand apelin. *J Biol Chem* **275:**21061–21067.

Ishida J, Hashimoto T, Hashimoto Y, Nishiwaki S, Iguchi T, Harada S, Sugaya T, Matsuzaki H, Yamamoto R, Shiota N, et al. (2004) Regulatory roles for APJ, a seven-transmembrane receptor related to angiotensin-type 1 receptor in blood pressure in vivo. *J Biol Chem* **279:**26274–26279.

Kagiyama S, Fukuhara M, Matsumura K, Lin Y, Fujii K, and Iida M (2005) Central and peripheral cardiovascular actions of apelin in conscious rats. *Regul Pept* **125:**55–59.

Lee DK, Cheng R, Nguyen T, Fan T, Kariyawasam AP, Liu Y, Osmond DH, George SR, and O'Dowd BF (2000) Characterization of apelin, the ligand for the APJ receptor. *J Neurochem* **74:**34–41.

Li JM, Gall NP, Grieve DJ, Chen M, and Shah AM (2002) Activation of NADPH oxidase during progression of cardiac hypertrophy to failure. *Hypertension* **40:**477–484.

Masri B, Knibiehler B, and Audigier Y (2005) Apelin signalling: a promising pathway from cloning to pharmacology. *Cell Signal* **17:**415–426.

Mikami A, Imoto K, Tanabe T, Niidome T, Mori Y, Takeshima H, Narumiya S, and Numa S (1989) Primary structure and functional expression of the cardiac dihydropyridine-sensitive calcium channel. *Nature* **340:**230–233.

Mitra A, Katovich MJ, Mecca A, and Rowland NE (2006) Effects of central and peripheral injections of apelin on fluid intake and cardiovascular parameters in rats. *Physiol Behav* **89:**221–225.

O'Carroll AM, Selby TL, Palkovits M, and Lolait SJ (2000) Distribution of mRNA encoding B78/apj, the rat homologue of the human APJ receptor, and its endogenous ligand apelin in brain and peripheral tissues. *Biochim Biophys Acta* **1492:** 72–80.

O'Dowd BF, Heiber M, Chan A, Heng HH, Tsui LC, Kennedy JL, Shi X, Petronis A, George SR, and Nguyen T (1993) A human gene that shows identity with the gene encoding the angiotensin receptor is located on chromosome 11. *Gene* **136:**355–360.

Reaux A, De Mota N, Skultetyova I, Lenkei Z, El Messari S, Gallatz K, Corvol P, Palkovits M, and Llorens-Cortès C (2001) Physiological role of a novel neuropeptide, apelin, and its receptor in the rat brain. *J Neurochem* **77:**1085–1096.

Reaux A, Gallatz K, Palkovits M, and Llorens-Cortes C (2002) Distribution of apelin-synthesizing neurons in the adult rat brain. *Neuroscience* **113:**653–662.

Seyedabadi M, Goodchild AK, and Pilowsky PM (2002) Site-specific effects of apelin-13 in the rat medulla oblongata on arterial pressure and respiration. *Auton Neurosci* **101:**32–38.

Sorli SC, van den Berghe L, Masri B, Knibiehler B, and Audigier Y (2006) Therapeutic potential of interfering with apelin signalling. *Drug Discov Today* **11:**1100–1106.

Sumners C, Myers LM, Kalberg CJ, and Raizada MK (1990) Physiological and pharmacological comparisons of angiotensin II receptors in neuronal and astrocyte glial cultures. *Prog Neurobiol* **34:**355–385.

Sun C, Du J, Raizada MK, and Sumners C (2003) Modulation of delayed rectifier potassium current by angiotensin II in CATH.a cells. *Biochem Biophys Res Commun* **310:**710–714.

Sun C, Li H, Leng L, Raizada MK, Bucala R, and Sumners C (2004) Macrophage migration inhibitory factor: an intracellular inhibitor of angiotensin II-induced increases in neuronal activity. *J Neurosci* **24:**9944–9952.

Szokodi I, Tavi P, Földes G, Voutilainen-Myllylä S, Ilves M, Tokola H, Pikkarainen S, Piuhola J, Rysä J, Tóth M, et al. (2002) Apelin, the novel endogenous ligand of the orphan receptor APJ, regulates cardiac contractility. *Circ Res* **91:**434–440.

Taheri S, Murphy K, Cohen M, Sujkovic E, Kennedy A, Dhillo W, Dakin C, Sajedi A, Ghatei M, and Bloom S (2002) The effects of centrally administered apelin-13 on food intake, water intake and pituitary hormone release in rats. *Biochem Biophys Res Commun* **291:**1208–1212.

Tatemoto K, Hosoya M, Habata Y, Fujii R, Kakegawa T, Zou MX, Kawamata Y, Fukusumi S, Hinuma S, Kitada C, et al. (1998) Isolation and characterization of a novel endogenous peptide ligand for the human APJ receptor. *Biochem Biophys Res Commun* **251:**471–476.

Tobin VA, Bull PM, Arunachalam S, O'Carroll AM, Ueta Y, and Ludwig M (2008) The effects of apelin on the electrical activity of hypothalamic magnocellular vasopressin and oxytocin neurons and somatodendritic peptide release. *Endocrinology* **149:**6136–6145.

Wang G, Anrather J, Huang J, Speth RC, Pickel VM, and Iadecola C (2004) NADPH oxidase contributes to angiotensin II signaling in the nucleus tractus solitarius. *J Neurosci* **24:**5516–5524.

Yin JX, Yang RF, Li S, Renshaw AO, Li YL, Schultz HD, and Zimmerman MC (2010) Mitochondria-produced superoxide mediates angiotensin II-induced inhibition of neuronal potassium current. *Am J Physiol Cell Physiol* **298:**C857–C865.

Yamazato M, Yamazato Y, Sun C, Diez-Freire C, and Raizada MK (2007) Overexpression of angiotensin-converting enzyme 2 in the rostral ventrolateral medulla causes long-term decrease in blood pressure in the spontaneously hypertensive rats. *Hypertension* **49:**926–931.

Zhang Q, Yao F, Raizada MK, O'Rourke ST, and Sun C (2009) Apelin gene transfer into the rostral ventrolateral medulla induces chronic blood pressure elevation in normotensive rats. *Circ Res* **104:**1421–1428.

Zimmerman MC, Lazartigues E, Lang JA, Sinnayah P, Ahmad IM, Spitz DR, and Davisson RL (2002) Superoxide mediates the actions of angiotensin II in the central nervous system. *Circ Res* **91:**1038–1045.

Address correspondence to: Dr. Chengwen Sun, Department of Pharmaceutical Sciences, North Dakota State University, P.O. Box 6050, Fargo, ND 58108-6050. E-mail: chengwen.sun@ndsu.edu